Društvo za tehniku
zavarivanja Slavonski Brod

12. Međunarodno znanstveno-stručno savjetovanje SBZ 2023

„STROJARSKE TEHNOLOGIJE U IZRADI ZAVARENIH KONSTRUKCIJA I PROIZVODA, SBZ 2023."
Slavonski Brod, 26. i 27.04.2023. i Požega 28.04.2023.

DETERMINATION OF OPTIMAL WELDING SEQUENCE FOR T-JOINT OF ALUMINIUM ALLOY BY NUMERICAL SIMULATIONS

Marko Mumović[1,*], Nikola Šibalić[1], Milan Vukčević[1], Darko Bajić[1]

[1]University of Montenegro, Faculty of Mechanical Engineering, Podgorica

[*] Corresponding Author. E-mail: marko.mumovic@ucg.ac.me

Abstract

The numerical optimization of the order of welding sequences at the T-joint was carried out in the paper, according to the criterion of minimum distortion of workpieces made of aluminum alloy AA6060. A T-joint with a single-sided seam was analyzed. The simulation was carried out, with a *Gas Metal Arc Welding* (GMAW) process, using a robotic arm, because this method allows the highest welding speed, and therefore the highest productivity. Due to numerous economic advantages, the application of *Al* alloys of the 6xxx series is widespread in the automotive, aviation, and railway industry, as well as in shipbuilding. Some of the advantages are a good ratio of weight to mechanical properties, resistance to corrosion, and easy recycling. The application of different sequences when welding workpieces can greatly affect the quality of the welded joint. This approach is particularly important at the T-joint, due to the appearance of rotation of a vertical member towards the side of the joint to be welded, as a result of the appearance of residual stresses during the cooling of the weld. Aluminum welding is even more difficult to control due to the high thermal conductivity of the material. Therefore, especially in the case of long welded joints, welding is not performed in one continuous pass but is welded and executed according to specific sequences. The goal of different strategies in the formation of sequences is primarily to obtain a high-quality welded joint with a minimal degree of distortion of the welded workpieces. The optimal strategy in this paper was adopted based on the results obtained by numerical simulation in the specialized *Computer Aided Engineering* (CAE) software Simufact Welding, which is based on the *Finite Element Method* (FEM). Input parameters of numerical simulations are presented in detail. The effects of temperature distribution and residual stresses were monitored as direct factors leading to distortion.

Keywords: Numerical Simulation, GMAW, T-joint, Aluminum Alloy, Welding Sequence

1. Introduction

The T-joint is a welded joint of two elements whose surfaces are approximately normal to each other in the region of the joint itself. This joint can be formed between two plates, a tube and a plate, or a tube and a cylindrical surface. The most common applications of this joint are when joining plates and branched structures. The vertical member of this joint can be joined using a corner seam. With a corner seam, the problem can appear in the form of a lack of full penetration. In dynamically loaded joints, an incomplete weld can act as an initial place for the appearance of a crack, especially in a T-joint that does not perform well under dynamic loads in operation. Therefore, in this paper, a proper care was taken to prepare workpieces that were welded using a single-sided fillet weld.

When designing new products, engineers strive to find the best balance between the mass and stiffness of components, with the lowest possible manufacturing costs. Because of these requirements, aluminum alloys excel in many engineering applications and are the material of choice for many products. Despite the development of the arc welding process, residual stresses and distortions caused by welding remain major obstacles in the production of lightweight structures. This is especially pronounced with thin plates. Since aluminum heats up locally very quickly, the internal temperature distribution is very uneven. This property, in combination with high heat conductivity and lower strength at elevated temperatures, leads to relatively high residual stresses and distortions, which can result in instability of mechanical characteristics and thus limit their application [1].

Arc welding is a complex process affected by many parameters, including electrical, kinematic, geometric, and many others, the combination of which can greatly affect welding distortions and residual stresses. In general, it is necessary to achieve a good welded joint, with as little heat input as possible. Performing real-world experiments to find optimal parameters is expensive and time-consuming, so this task can be solved using welding simulation software [2].

One of the main methods of improving the quality of the joint, which is primarily used for long welds, is the division of the weld into segments [3]. Welding these segments in a certain order makes a sequence. Optimizing the order of execution of these segments can greatly influence the minimization of negative features that accompany the welding process. With the development of computer technology and numerical methods of solving equations, numerical simulations have been widely used in the simulation of numerous production processes, including welding. In welding, these simulations are used to predict welding temperature, residual stress, and distortion [4].

2. Mathematical Model

CAE software Simufact Welding includes process and material structure simulation. This software uses a mathematical model of heat propagation, which can simulate any electric arc process through the appropriate geometry of the heat source [5]. Modeling the heat source is the most difficult challenge in the simulation of the heat distribution field, which directly affects the quality of the welded joint. To simulate heat sources in arc welding processes, the software uses the Goldak heat

source model. Goldak's heat source model, a double ellipsoid, is a volume model [6] that most faithfully represents the heat source during electric arc welding. This geometry is made up of the quadrants of two different ellipsoids. Calculations showed that the temperature gradient under the heat source is not as steep as the gradient on the following side, so it is described by two ellipsoids with different parameters [7]:

$$q_f=q(x,y,z)=\frac{6\sqrt{3}f_f\dot{Q}}{abc_f\pi\sqrt{\pi}}e^{-3x^2/a_f^2}e^{-3y^2/b^2}e^{-3z^2/d^2} \quad (1)$$

$$q_r=q(x,y,z)=\frac{6\sqrt{3}f_r\dot{Q}}{abc_r\pi\sqrt{\pi}}e^{-3x^2/a_r^2}e^{-3y^2/b^2}e^{-3z^2/d^2} \quad (2)$$

In expressions (1) and (2), f_f are f_r are the fractions of heat flux in the front and rear quadrants where $f_f+f_r=2$, a_f, a_r, b, d are geometric parameters that define the size and shape of the ellipsoid, and therefore the distribution of heat. The geometrical parameters are independent and can have different values, for example with heterogeneous materials, Goldak's heat source would consist of four octants, with different values of the geometrical parameters [6].

Since the temperature of the material during welding is variable, the case of a three-dimensional non-stationary heat transfer problem arises. For the considered case of welding and heat generation, this problem can be described by the Fourier equation of heat:

$$\frac{\partial T}{\partial t}=\alpha\nabla^2 T+\dot{Q} \quad (3)$$

$$\frac{\partial}{\partial x'}\left(\frac{k}{\rho c}\frac{\partial T}{\partial x'}\right)+\frac{\partial}{\partial y'}\left(\frac{k}{\rho c}\frac{\partial T}{\partial y'}\right)+\frac{\partial}{\partial z'}\left(\frac{k}{\rho c}\frac{\partial T}{\partial z'}\right)=\frac{\partial T}{\partial t}+\dot{Q} \quad (4)$$

where: T – temperature, k – coefficient of thermal conductivity, ρ – material density, c – specific heat of the workpiece material, $\alpha=k/\rho c$ – thermal diffusivity, x' – direction along the welded joint y' – direction of the cross-section, z' – direction along the thickness of the workpiece, Q – heat from the source and t – time.

Assuming that the dimensions of the heat source are far smaller than the workpiece, we can adopt the approximation that the heat source is of the point type. Except at the beginning and end of the welding process, the temperature distribution in the workpiece is stationary as viewed from the moving coordinate system located in the heat source and moving along with it. Under such conditions, the time variable in the process disappears and the process is reduced to a quasi-stationary process, which allows to conduct given substitution and observe the problem from a moving coordinate system [8]:

$$x=x'-vt;\ y=y';\ z=z' \quad (5)$$

where: v – speed of the moving heat source. We transform the temporal dependence into a spatial:

$$\frac{\partial T}{\partial t}=\frac{\partial T}{\partial x}\frac{dx}{dt}=-v\frac{\partial T}{\partial x} \tag{6}$$

By adopting new variables, the initial equation is transformed into [9]:

$$\frac{k}{\rho c}\left(\frac{\partial^2 T}{\partial x^2}+\frac{\partial^2 T}{\partial y^2}+\frac{\partial^2 T}{\partial z^2}\right)+v\frac{\partial T}{\partial x}=\dot{Q} \tag{7}$$

The heat coming from the heat source is obtained based on Joule's law:

$$\dot{Q} = U \cdot I \cdot \eta \tag{8}$$

where: U – welding voltage, I – welding current, and η – efficiency of the electric arc.

3. Preparation of workpieces

As the workpieces that make up the T-joint, two plates made of aluminum alloy AA6060, thickness $t = 4$ mm were taken as where the dimensions of the vertical member are $a_1 = 150$ mm and $b_1 = 1000$ mm, and the dimensions of the horizontal member are $a_2 = 300$ mm and $b_2 = 1000$ mm. This type of welded joint is found on the welded structures of high-speed train carts [4]. The workpieces are welded along the longer side, i.e. the length of the welded joint is $l = 1000$ mm.
Based on the adopted dimensions of the workpieces, a *Computer Aided Design* (CAD) model was created that serves as the basis for generating a mesh of finite elements. The recommended mesh for this software is hexahedral [5] and to get the best simulation results, the generated mesh is also conformal. The formed mesh for the workpieces as well as the weld profile is given in Figure 1.

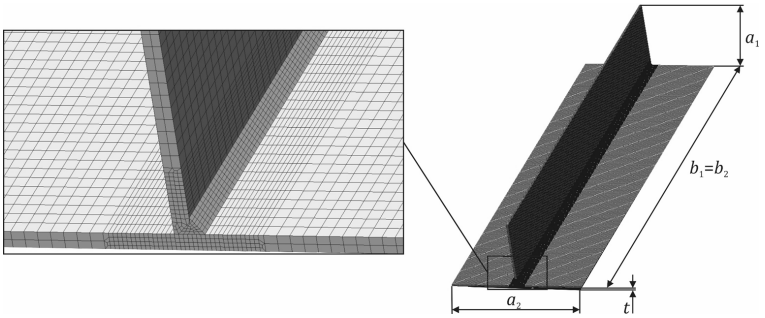

Figure 1. Workpieces with generated mesh

The mesh of finite elements in the that directly enters the welded joint consists of a finer mesh, the size of which in the section is 1 x 1 mm, and in the along the welded joint (*y-axis*) is 4 mm. This region has a width of 15 mm on the vertical piece and a width on a horizontal piece of 30 mm. The rest of the mesh is made of larger elements (coarse mesh) with a size of 2 x 3 mm in cross-section, and along the welded joint its size is also 4 mm. There is a transition region between the coarse and fine mesh of 1.25 mm.

4. Numerical experiment

For both workpieces, the material AA6060-T4 was assigned, and the alloy AA5356 was adopted as a filler material. For clamping the workpieces, 8 clamps of circular cross-sections with a diameter of 50 mm are used, which are located on the upper side, and each clamp the workpieces with a force of 200 N (Figure 2).

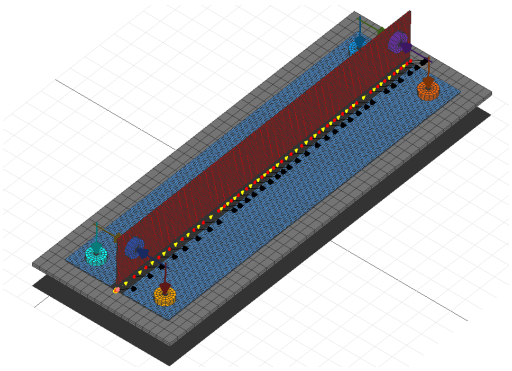

Figure 2. Workpieces with mechanical constraints

Although the software allows the removal of clamps at a certain point in the simulation, it is adopted that they are active during the entire welding and cooling process, which corresponds to the application in real-world conditions. The convective heat transfer coefficient is taken for the case of free convection in air $h = 20$ W/(m^{2}K) [9].
Since the heat conduction coefficient of the bodies in contact, among other factors, also depends on the pressure between the contact surfaces, an automatic calculation is selected in the software (offered option). For the emissivity coefficient, the value for aluminum plate $\varepsilon = 0.09$ is taken [10].
A seam with a flat face was chosen to perform the process (Figure 3).

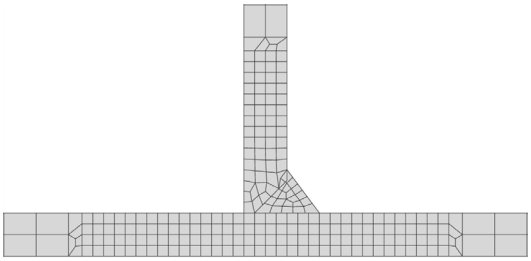

Figure 3. Fillet weld profile

It was automatically generated in the simulation software itself, where it was necessary to enter the following values: weld leg one is 6 mm and weld leg two is 5 mm, the face of the weld (concavity and convexity) is zero, *mesh quality – fine*, and the software automatically calculates the throat size is 3.84 mm. The moving heat source in these simulations is a double ellipsoid, i.e. the Goldak model (Figure 4), which is defined by the following parameters, which are defined in Table 1.

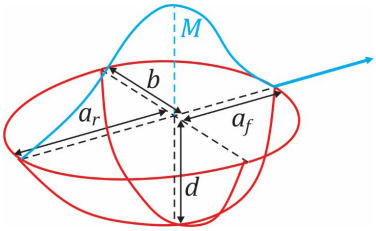

Figure 4. Goldak's heat source model [1]

Geometric parameters are identified experimentally, most often by micrographic analysis of the welded joint, however, if this value is not available, which is the case in this paper, it can be approximated according to certain laws [5]. The value of M is dimensionless and represents the Gaussian parameter of energy distribution over the surface. The choice of welding parameters was made for the GMAW process of aluminum with a thickness of $t = 4$ mm [4].
Basic parameters and welding parameters for the simulation are given in Table 1.
The process efficiency η is adopted according to [11].

Table 1. Adopted numerical simulation welding parameters

Basic parameters	
Welding process	GMAW
Ambient temperature	20°C
Gravity	9.81 m/s^2
Gravity direction	z:-1
Components	2
Bearings	1
Clampings	8
Robotic arm	1
Component material	AA6060-T4
Filler material	AA5356
Convective coefficient - h	20 W/(m^{2}K)
Conductive heat coefficient - a	Automatic
Emission coefficient - ε	0.09

Welding parameters	
Welding voltage U	20 V
Welding current I	140 A
Efficiency η	0.85
Welding speed v	6 mm/s
Parameters of the Goldak model	
Front length a_f	3.63 mm
Rear length a_r	13.31 mm
Width b	6.05 mm
Depth d	6.55 mm
Gaussian parameter M	3

Based on the adopted parameters, the amount of heat input is obtained to be 3966.7 J/mm.

5. Welding Sequences

In the process of electric arc welding, the metal is heated locally, and the deformation of the heated zone is prevented by the surrounding cold metal. This creates stresses greater than the material's

elastic limit (R_e) and causes permanent distortion. The level of distortion caused by the welding process is influenced by several factors: properties of the base material, clamping, joint design, edge preparation, and the welding process itself.

Regarding welding procedures, the general rule for reducing distortion is to have a minimum volume of melted material in as few passes as possible, but also to balance the contraction forces around the neutral axis of the workpieces and use segmental welds instead of continuous ones, i.e. segmentation of welds [3]. Another very important distortion control technique is the welding sequence, which is the subject of this paper. Four strategies will be tested, the first one is continuous welding, which also serves as a reference case. The second strategy is the *Back-step* where the welds are divided into short segments that are welded in the opposite direction of the general weld progression. For example, if the weld progresses from left to right, the weld segments are performed from right to left. Another strategy is *Skip-stop* welding. The welding direction is the same as in *Back-step* welding, with the exception that the welding of segments is not performed in a continuous sequence. For example, the first is welded, the second is skipped, then the third weld is performed, etc. The fourth strategy is welding from the middle of the workpieces to the ends - *From center*. Based on the selected variations, we obtain a numerical experiment with four experimental points according to Table 2.

Table 2. Experimental plan for welding

Sequence nr.	Sequence strategy	Sequence order
Sequence 1	None	+1,+2,+3,+4
Sequence 2	Back-step	-1,-2,-3,+4
Sequence 3	Skip-stop	-1,-3,+4,-2
Sequence 4	From center	-2+3,-1,+4

For the sake of simplicity of segment direction markings, the "-" sign is adopted before the segment number and indicates the direction opposite to the welding progression, and the "+" sign before the segment number, the same direction as the welding progression. It should be noted that when continuing each new sequence, the electric arc is started on the already formed seam at a length of about 12 mm, which prevents the appearance of crater defect. Figure 5 shows the scheme of the welded joint with adopted four segments, the order of which varies in numerical simulations.

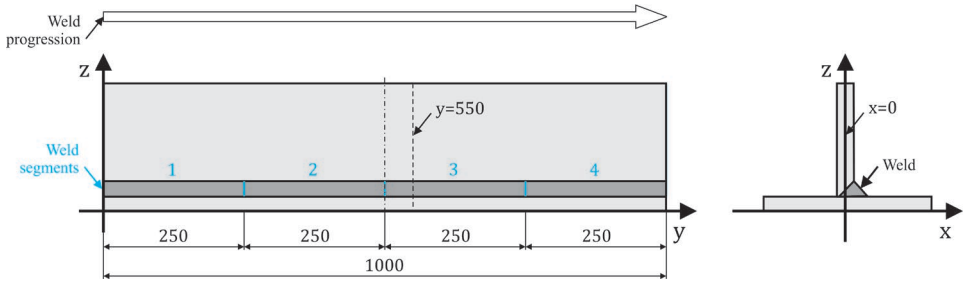

Figure 5. Welding segments

6. Results and Discussion

After the past 500 seconds of the simulation duration, the workpieces at all points have been cooled to a temperature that is not higher than 25 °C compared to the ambient temperatures, so it can be considered that the distortion process is slightly progressing and that any further extension of process tracking will only result in a simulation whose execution will last longer, and there will be no change in the order of the sequences. It can be seen from Figure 6 that the best result, i.e. the lowest value of distortion, is obtained for welding segments with the *From center* strategy in Sequence 4, and the highest value of distortion is obtained in Sequence 3.

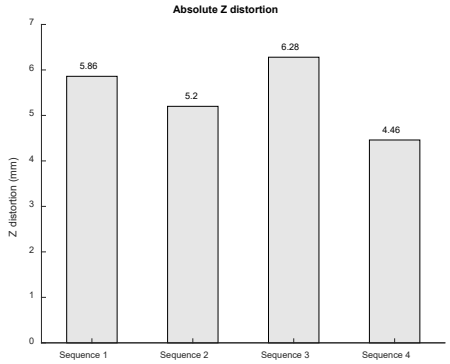

Figure 6. Absolute distortion results along the z-axis

If we compare these values of Sequence 1, where we have a continuously welded joint without breaks, with Sequence 4, we get that the z-axis distortion is ≈ 31% higher, which indicates the positive effects of this approach. Also, it turns out that the distortion of Sequence 3 compared to Sequence 4 along the z-axis is ≈ 41% higher. Distortion as a phenomenon in electric arc welding is a direct consequence of the appearance of internal stresses in the welding zone that are caused by a sudden change in the temperature of the material that comes from the heat introduced by the electric arc. Therefore, when examining welding distortion, the most important parameters are the residual stresses and the highest temperatures that occur in the material. The residual stress and temperature results are given in the cross-section (Figure 7 and 9) and the longitudinal section (Figure 8 and 10). The position of the cross-section is in the Segment 3 defined on Figure 5 by plane y=550, in other words at distance of 50 mm from the beginning of the segment, in order not to observe the section where the electric arc crossed the material twice during the starting of the arc for the new segment. Position of the longitudinal section is in the middle of T-joint defined on Figure 5 by plane x=0. The values of the residual stresses were compared for the test cases of Sequence 1 and Sequence 4 of the experimental plan, wherein the cross-section (Figure 7) a large value of the residual stresses is obtained in the central part, after which there is a drop in the value of the residual stresses with distance from the center, and then until the appearance of two smaller peaks when leaving the heat-affected zone (HAZ). The peaks are more pronounced in Sequence 1, compared to Sequence 4. In the longitudinal

section (Figure 8), the peaks appear at the beginning and end of the welded joint, as well as at the arc starting points during segmentation.

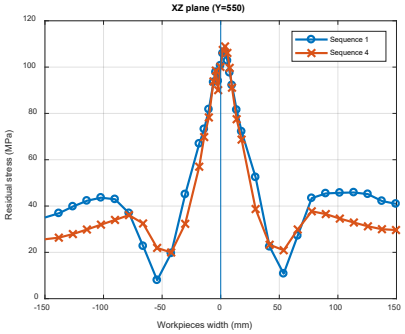

Figure 7. Comparative values of residual stresses in the cross-section

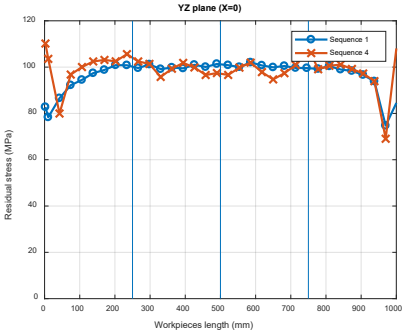

Figure 8. Comparative values of the residual stresses in the longitudinal section

As the distance from the weld increases, the maximum temperature value when comparing the extreme values of the sequences gradually decreases in the cross-section (Figure 9) and these values are approximate for both sequences. For sequence 4, we can observe irregularities in the temperature distribution in the longitudinal section (Figure 10), which is conditioned by the chosen strategy of making the segments.

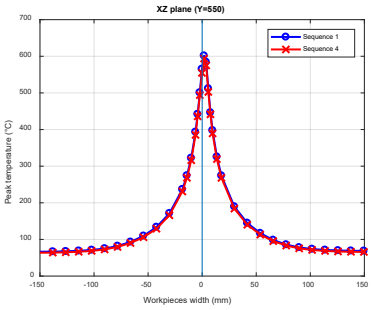

Figure 9. Comparative values of the maximum temperature in the cross-section

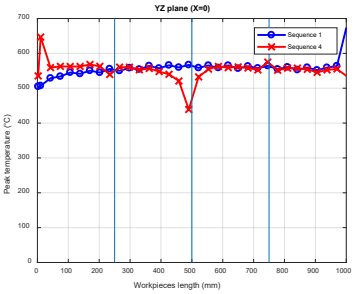

Figure 10. Comparative values of maximum temperature by longitudinal section

Figure 11 shows the values of distortion and residual stresses for each experimental point. The residual stress values are shown in two views.

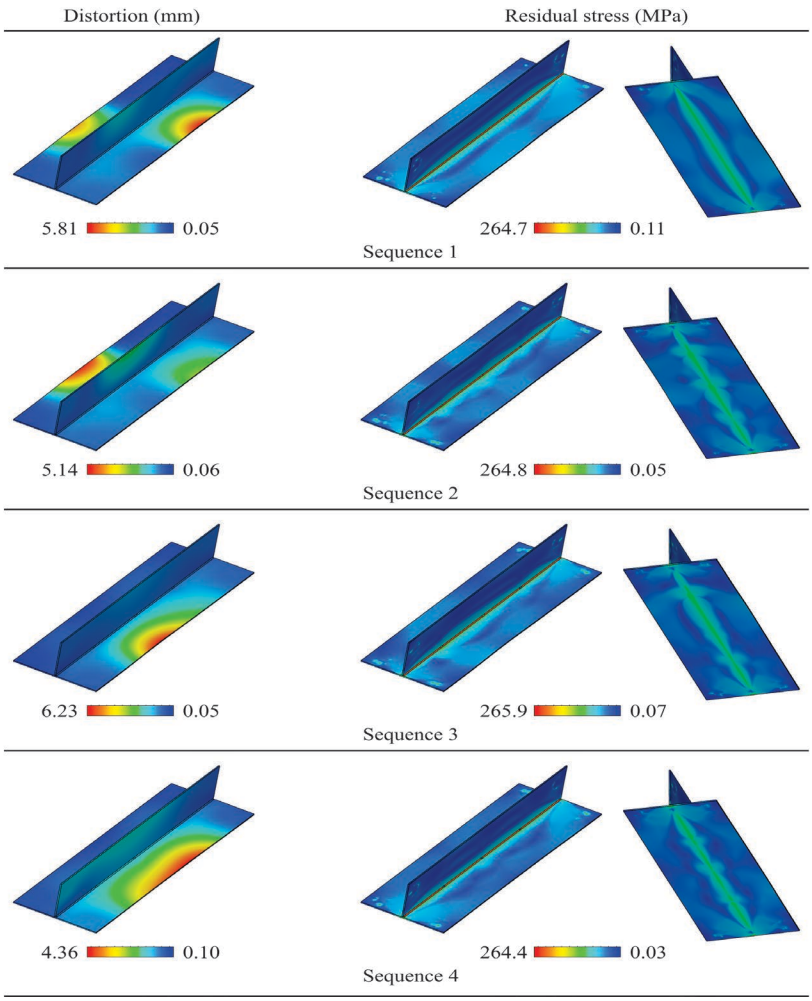

Figure 11. Values of distortion and residual stress for each experimental point

We can observe great differences in the localization of distortion and its intensity depending on the segmentation execution strategy, as well as the appearance of characteristic forms of stress distribution.

7. Conclusion

Distortion of welded structures is an inevitable side effect, but it can be significantly reduced by an adequate choice of welding parameters and the application of an appropriate segmentation strategy. Based on the experimental plan, the paper analyzed four different strategies using numerical simulations for a one-sided T-joint. The values of the residual stresses after cooling the workpieces and the maximum temperature reached by the material were monitored as the most influential parameters on distortion. These values were monitored in longitudinal and cross-section. The biggest difference in results occurs in the longitudinal section. No significant differences in values can be

observed for the cross-section. A difference of about 41% was observed between the results of the best and worst strategies. This phenomenon becomes more pronounced with increasing weld length. It is also shown that numerical simulations can be used as a very useful tool for distortion prediction and this approach can be applied to a wide class of welding problems.

ACKNOWLEDGMENTS

The authors hereby thank MSC. Software GmbH for providing the use of the licensed Simufact Welding software.

8. References

[1] Mumović, Marko; Šibalić, Nikola; Bajić, Darko; Vukčević, Milan. (2021). Numerical Analysis of Welding Sequence Influencing the Quality of an AA6060-T4 Alloy Lap Joint. S*tructural Integrity and Life, Vol.* 21*, No.* 2*,* 123–130.

[2] Khoshroyan, Amirreza; Darvazi, Armin, Rahmati. (2020). Effects of welding parameters and welding sequence on residual stress and distortion in Al6061-T6 aluminum alloy for T-shaped welded joint. *Trans. Nonferrous Met. Soc. China English Ed., Vol.* 30*, No.* 1*,* 76–89.
doi: 10.1016/S1003-6326(19)65181-2.

[3] Romero-Hdz, Jesus; Toledo-Ramirez, Gengis; Saha, Baidya. (2017). Deformation and Residual Stress Based Multi-Objective Genetic Algorithm for Welding Sequence Optimization. *Res. Comput. Sci., Vol.* 132*, No.* 1*,* 155–179*,* doi: 10.13053/rcs-132-1-12.

[4] Lu, Yaohui; Zhu, Shengchang; Zhao, Zhitang; Chen, Tianli; Zeng, Jing. (2020). Numerical simulation of residual stresses in aluminum alloy welded joints. J. *Manuf. Process., Vol.* 50, 380–393, doi: 10.1016/j.jmapro.2019.12.056.

[5] Welding simulation Simufact Welding - Simufact software solutions. https://www.simufact.com/simufactwelding-welding-simulation.html (accessed Jan. 10, 2021).

[6] Goldak, John; Chakravarti, Aditya; Bibby, Malcolm. (1984). A New Finite Element Model for Welding Heat Sources. *Metall. Trans. B, Vol. 15B, No.* 1*,* 1–7*,*
doi: 10.1080/21681805.2017.1363816.

[7] Farias, R. M.; Teixeira, P. R. F.; Vilarinho, L. O. (2020). An efficient computational approach for heat source optimization in numerical simulations of arc welding processes. *J. Constr. Steel Res., Vol.* 176*,* doi: 10.1016/j.jcsr.2020.106382.

[8] Yeh, Rong-Hua; Liaw, Shih-Pin; Yu, Hong-Bin. (2003). Thermal analysis of welding on aluminum plates. *Journal of Marine Science and Technology, Vol.* 11*, No.* 4*,* 213–220.

[9] Convection Heat Transfer Coefficient - an overview - ScienceDirect Topics, Exploring Engineering. https://www.sciencedirect.com/science/article/pii/B9780124158917099982
(accessed Apr. 22, 2021).

[10] Emissivity Coefficient Materials," Engineering ToolBox, 2003.
https://www.engineeringtoolbox.com/emissivity-coefficients-d_447.html
(accessed Apr. 22, 2021).

[11] Pepe, Nuno; Egerland, Stephan; Colegrove, Paul A.; Yapp, David; Leonhartsberger, Andreas; Scotti, Americo. (2011). Measuring the process efficiency of controlled gas metal arc welding processes. *Science and Technology of Welding and Joining, Vol.* 16*, No.* 5, 412–417,
doi: 10.1179/1362171810Y.0000000029.